Bone Reports 5 (2016) 312–319

Contents lists available at ScienceDirect

Bone Reports

journal homepage: www.elsevier.com/locate/bonr

Bone microstructure in men assessed by HR-pQCT: Associations with risk factors and differences between men with normal, low, and osteoporosis-range areal BMD

Narihiro Okazaki, M.D., Ph.D. [a,b,*], Andrew J Burghardt, B.S. [a], Ko Chiba, M.D., Ph.D. [b], Anne L Schafer, M.D. [c,d,e], Sharmila Majumdar, Ph.D. [a]

[a] Department of Radiology and Biomedical Imaging, University of California, San Francisco, USA
[b] Department of Orthopaedic Surgery, Nagasaki University Graduate School of Biomedical Sciences, Japan
[c] Medical Service, San Francisco VA Medical Center, USA
[d] Department of Medicine, University of California, San Francisco, USA
[e] Department of Epidemiology and Biostatistics, University of California, San Francisco, USA

ARTICLE INFO

Article history:
Received 8 July 2016
Received in revised form 12 October 2016
Accepted 30 October 2016
Available online 2 November 2016

Keywords:
Male osteoporosis
HR-pQCT
Aging
Cortical porosity
Cortical bone

ABSTRACT

Purpose: The primary objective of this study was to analyze the relationships between bone microstructure and strength, and male osteoporosis risk factors including age, body mass index, serum 25-hydroxyvitamin D level, and testosterone level. A secondary objective was to compare microstructural and strength parameters between men with normal, low, and osteoporosis-range areal bone mineral density (aBMD).
Methods: Seventy-eight healthy male volunteers (mean age 62.4 ± 7.8 years, range 50–84 years) were recruited. The participants underwent dual-energy X-ray absorptiometry (DXA) and high-resolution peripheral quantitative computed tomography (HR-pQCT) of the ultra-distal radius and tibia. From the HR-pQCT images, volumetric bone mineral density (BMD) and cortical and trabecular bone microstructure were evaluated, and bone strength and cortical load fraction (Ct.LF) were estimated using micro-finite element analysis (μFEA).
Results: Age was more strongly correlated with bone microstructure than other risk factors. Age had significant positive correlations with cortical porosity at both ultra-distal radius and tibia ($r = 0.36$, $p = 0.001$, and $r = 0.47$, $p < 0.001$, respectively). At the tibia, age was negatively correlated with cortical BMD, whereas it was positively correlated with trabecular BMD. In μFEA, age was negatively correlated with Ct.LF, although not with bone strength. Compared with men with normal aBMD, men with low or osteoporosis-range aBMD had significantly poor trabecular bone microstructure and lower bone strength at the both sites, while there was no significant difference in cortical bone.
Conclusions: Cortical bone microstructure was negatively affected by aging, and there was a suggestion that the influence of aging may be particularly important at the weight-bearing sites.

1. Introduction

Osteoporosis is a serious health problem not only in women but also in men. According to the National Osteoporosis Foundation, about one out of two women and one out of four men over 50 years old will have an osteoporosis-related fracture in their remaining lifetime (National Osteoporosis Foundation, 2002). While the incidence rate is lower in men, men with osteoporosis-related fracture have higher morbidity and mortality rates than women (Center et al., 1999; Morin et al., 2010). As the average age of the population continues to increase, the incidence of male osteoporosis is expected to increase significantly. Although many studies of prevention and treatment have been performed in recent years, the pathogenesis of skeletal fragility in men remains unclear.

High-resolution peripheral quantitative computed tomography (HR-pQCT) is a noninvasive approach which enables in vivo 3D analysis of bone microstructure at the appendicular skeleton (Laib et al., 1998; Müller et al., 1996); this allows the analysis of geometric, microstructural, densitometric, and mechanical properties of the trabecular and cortical bone architecture in the distal radius and tibia (Burghardt et al., 2007; Boyd, 2007). In addition, the application of micro finite-element (μFE) analysis permits the estimation of bone strength (Boyd, 2008). How these microstructural and strength parameters relate to areal bone mineral density (BMD) in men is unclear. Further, it is unclear how microstructural and strength parameters are affected by male

* Corresponding author at: 1-7-1 Sakamoto, Nagasaki 852-8501, Japan.
E-mail address: n.okazaki@nagasaki-u.ac.jp (N. Okazaki).

http://dx.doi.org/10.1016/j.bonr.2016.10.005

osteoporosis risk factors including advanced age, low body weight, physical inactivity, hypogonadism, heavy smoking, excessive alcohol consumption, vitamin D deficiency, and inadequate calcium intake (Papaioannou et al., 2008; Ebeling, 2008; Bartl and Frisch, 2009).

In this study, we used HR-pQCT to determine bone microstructure and strength at the distal radius and tibia in 78 older men. (1) We analyzed the relationships between bone microstructure and strength, and male osteoporosis risk factors including age, body mass index (BMI), 25-hydroxyvitamin D (25(OH)D) level, and testosterone level. In addition, we estimated 10-year fracture risk using the fracture risk assessment tool (FRAX) (World Health Organization, 1994) and analyzed the relationships between bone microstructure and FRAX score. (2) Finally, we compared bone microstructure and strength measures of men with normal, low, and osteoporosis-range areal BMD (aBMD).

2. Materials and methods

2.1. Subjects

The subjects consisted of 78 healthy male volunteers. The recruitment was done using electronic kiosk announcements and flyers posted in the San Francisco VA Medical Center (San Francisco, USA), and weekly internet advertisements. We excluded men who had been treated with either an oral bisphosphonate or teriparatide in the last year or for >12 months ever, and those who had diseases or took medications known to affect bone metabolism, including current use of testosterone therapy, and use of prednisone >5 mg daily or the equivalent glucocorticoid for >10 days in the last 3 months. Other exclusion criteria included alcohol use >3 drinks/day, serum calcium level > 10.2 mg/dL, and estimated glomerular filtration rate < 30 mL/min/1.73m^2.

The study protocol was approved by the UCSF Committee on Human Research and complied with the Declaration of Helsinki of 1975, revised in 2000, and written informed consent was obtained before participation.

2.2. Biochemical measurements

Blood samples were collected from all subjects. Serum calcium and creatinine levels were measured on the Beckman Coulter (Fullerton, CA) DXC800 instrument using a Synchron assay. 25(OH)D was measured by electrochemiluminescent immunoassay (DiaSorin LIAISON). Serum total testosterone was determined using the Access testosterone assay (Beckman Coulter).

2.3. Areal bone mineral density and FRAX

Areal BMD (aBMD) was measured by dual-energy X-ray absorptiometry (DXA) (GE Lunar DXA, GE Healthcare Systems, Wauwatosa, WI, USA) at the lumbar spine (L1 to L4), non-dominant hip (total hip and femoral neck), and radius (distal one-third, ultra distal, and total).

The 10-year probabilities of major osteoporotic fracture (hip, proximal humerus, distal radius, or clinical spine fracture) and hip fracture were estimated using FRAX (version 3.9).

2.4. HR-pQCT and image-based μFEA of the ultra-distal radius and tibia

All subjects were imaged in a clinical HR-pQCT system (XtremeCT, Scanco Medical AG, Brüttisellen, Switzerland) using the manufacturer's standard in vivo protocol described in previous patient studies (Sornay-Rendu et al., 2007; Kazakia et al., 2008; Melton et al., 2007). The subject's forearm and ankle were immobilized in a carbon fiber cast that was fixed within the gantry of the scanner. A single dorsal-palmar projection image of the distal radius and tibia was acquired to define the tomographic scan region. This region spanned 9.02 mm in length (110 slices) and was fixed starting proximally at 9.5 and 22.5 mm from a joint margin reference line for ultra-distal radius (UDR) and ultra-distal tibia (UDT), respectively. For tomography, 750 projections were acquired over 180 degrees with a 100-ms integration time at each angular position. The 12.6-cm field of view (FOV) was reconstructed across a 1536 × 1536 matrix using a modified Feldkamp algorithm, yielding 82-μm voxels (Feldkamp et al., 1984). Total scan time was 2.8 min with an equivalent dose of approximately 4.2 μSv for each site.

2.5. Image analysis

2.5.1. Image quality grading for motion artifacts

The severity of motion artifacts was graded according to the manufacture-suggested image quality grading system. Grading was performed in 3 slices (at the middle and both proximal and distal end slices) of the reconstructed images, and the images with grades 4 and 5 were excluded (Pialat et al., 2012). One case in UDR was excluded due to motion artifact. Therefore, 77 cases of UDR and 78 cases of UDT were available for analysis.

2.6. Standard analysis

All image analysis was performed using the standard clinical evaluation protocol in Image Processing Language (IPL Version 5.08b, Scanco Medical AG), as described in detail in previous publications (Kazakia et al., 2008; Tjong et al., 2012). Contours identifying the periosteal perimeter of the bone were drawn semiautomatically using a chaperoned iterative contouring procedure. All contours were examined manually and modified as necessary to delineate the periosteal boundary. Integral volumetric BMD was quantified based on the periosteal segmentation. A threshold-based process was used to segment cortical and trabecular regions for compartment-specific measurements of density and structure (Laib et al., 1998). Trabecular bone volume fraction (BV/TV) was calculated based on trabecular BMD (Tb.BMD) assuming a tissue mineral density of 1200 mg HA/cm^3. Trabecular number (Tb.N) was calculated directly by a model-independent sphere fitting technique (Hildebrand et al., 1999; Laib et al., 1997). Based on the calculated BV/TV and Tb.N values, trabecular separation (Tb.Sp) and trabecular thickness (Tb.Th) were derived using standard histomorophometric relations assuming a plate model (Laib and Rüegsegger, 1999).

2.7. Cortical analysis

Cortical bone microstructure parameters at ultra-distal sites were assessed using an extended cortical bone analysis that provides direct calculation of cortical thickness, as well as measures of porosity (Buie et al., 2007; Burghardt et al., 2010). Values for the following structural parameters were calculated: cortical BMD (Ct.BMD), cortical thickness (Ct.Th), cortical porosity (Ct.Po), and cortical pore diameter (Po.Dm). Ct.BMD was calculated as the mean value of all voxels within the cortical compartment, following partial volume suppression (2 voxels) at the periosteal and endosteal surfaces. Ct.Po was defined as the fraction of the segmented pore volume over the sum of the pore and cortical bone volume.

2.8. Micro-finite element analysis (μFEA)

Linear μFEA was used to calculate apparent biomechanical properties at each site. Homogeneous mechanical properties were assumed for all bone elements. The binary image data set was converted to a mesh of voxels (isotropic) using a conversion technique (Müller and Rüegsegger, 1995), and each element was assigned an elastic modulus of 6.829 GPa (Boyd, 2008) and a Poisson's ratio of 0.3 (van Rietbergen et al., 1996). Cortical and trabecular bone elements were labeled as different materials, with identical material properties to facilitate calculation of compartmental load distribution. A uniaxial compression test in the axial direction (superior-inferior) was performed with an applied

uniaxial compressive strain of 1%. An iterative solver (Scanco FE software v.1.15; Scanco Medcal AG, Brüttisellen, Switzerland) was used to compute reaction forces at the proximal and distal ends of the scan region for the proscribed displacements. For each model, stiffness (K), apparent modulus (E), and the load fraction for the cortical compartment at the distal boundary (Ct.LF dist) and the proximal boundary (Ct.LF prox) were calculated. Furthermore, failure load (F) was estimated using methods previously described by Mueller et al. (2011).

2.9. Statistical analysis

Statistical analyses were performed using SPSS version 16.0 (SPSS, Chicago, IL, USA).

(1) The relationships between the bone microstructure and μFEA parameters, and age, BMI, 25(OH)D, and testosterone were analyzed by Pearson's correlation coefficient test. The relationships between the bone microstructure and μFEA parameters, and FRAX score (the 10-year probability of a major osteoporotic fracture and of a hip fracture) were analyzed in the same way. The level of statistical significance was established at $p < 0.05$.
(2) All subjects were classified as having normal, low, or osteoporosis-range BMD according to World Health Organization (WHO) categories based on DXA T-score at lumbar spine, total hip and femoral neck: normal aBMD if lowest T-score ≥ −1.0; low bone mass ("osteopenia") if −2.5 < T-score < −1.0; osteoporosis if T-score ≤ −2.5 (World Health Organization, 1994). We compared the bone microstructure and μFEA parameters between the normal group and osteopenic or osteoporotic groups. A Bonferroni correction was used to account for multiple comparisons, therefore the level of statistical significance was set at $p < 0.025$.

3. Results

The mean age of 78 subjects was 62.4 ± 7.8 years (range 50–84 years). Forty-four men (56%) were white, 18 (23%) were African American, 11 (14%) were Asian, 4 (5%) were Hispanic, and 1 (1%) was American Indian. The mean BMI was 27.1 ± 3.2 kg/m^2, testosterone was 423.2 ± 165.1 ng/dL, and 25(OH)D level was 23.2 ± 9.6 ng/mL. Trabecular and cortical bone microstructure parameters and μFEA parameters at UDR and UDT are displayed in Table 1, with representative 3D images of cortical bone in Fig. 1.

Table 1
Bone microstructure and μFEA parameters of the ultra distal radius and the ultra distal tibia.

Parameter	Radius (n = 77)				Tibia (n = 78)			
	Mean	SD	Min	Max	Mean	SD	Min	Max
Tb.Th (μm)	75	11	53	101	79	12	52	108
Tb.N (/mm)	2.00	0.28	1.36	2.46	1.94	0.31	1.21	2.66
Tb.Sp (μm)	434	76	320	651	448	88	294	725
Tb.BMD (mg/cm^3)	181	37	104	258	184	35	109	263
Ct.Th (mm)	0.97	0.17	0.61	1.53	1.40	0.26	0.89	2.21
Ct.Po (%)	2.9	1.3	1.1	8.2	7.0	2.6	1.9	16.7
Po.Dm (μm)	172	21	143	240	191	23	152	307
Ct.BMD (mg/cm^3)	924	45	735	1017	881	55	735	1001
Stiffness, *K* (kN/mm)	68.6	13.1	38.6	105.3	172.8	30.2	103.7	281.4
Modulus, *E* (N/m^2)	1290	285	696	1985	1614	304	861	2186
Failure load, *F* (N)	4057	726	2350	6176	9982	1697	6275	16112
Ct.LF-dist (%)	41.2	7.4	28.7	67.1	44.1	7.3	28.0	62.5
Ct.LF-prox (%)	79.1	5.8	63.3	90.9	66.6	6.9	50.0	84.9

3.1. The relationships between bone microstructure parameters and risk factors of male osteoporosis.

BMI was significantly correlated with total hip, femoral neck, total radius, and 1/3 radius T-scores by DXA, such that those with higher BMI had higher DXA T-scores (Table 2). By HR-pQCT, at the UDR, age had a significant positive correlation with Ct.Po ($r = 0.36$, $p = 0.001$, Table 2, Fig. 2), such older participants had greater cortical porosity. At the UDT, age was positively correlated with Ct.Po ($r = 0.47$, $p < 0.001$, Table 2, Fig. 2) and negatively correlated with Ct.BMD ($r = -0.40$, $p < 0.001$), whereas it was positively correlated with Tb·BMD ($r = 0.30$, $p = 0.008$). BMI was correlated with Tb.N, Tb.Sp, and Ct.Th at UDT, such that those with higher BMI had higher Tb.N, lower Tb.Sp, and higher Ct.Th. Cortical porosity was increased significantly with aging, particularly at the UDT. In addition, age was negatively correlated with Ct.LF-prox and Ct.LF-dist ($r = -0.48$, $p < 0.001$ and $r = -0.36$, $p = 0.001$, respectively). Age was not correlated with stiffness, apparent modulus, or failure load.

At the UDR, those with lower Tb.BMD, Ct.BMD, and Ct.Th, and higher Ct.Po had higher FRAX scores for major osteoporotic fracture; those with lower Tb.BMD and Tb.N, and higher Tb.Sp and Ct.Po had higher FRAX scores for hip fracture. On the other hand, at the UDT, those with lower Ct.BMD and Ct.Th had higher FRAX score for major osteoporotic fracture and hip fracture; those with lower Tb.BMD had also higher FRAX score for hip fracture. At both the UDR and UDT, those with lower stiffness, apparent modulus, and failure load had higher FRAX score for major osteoprotic fracture and hip fracture, such that those with lower estimated bone strength had higher FRAX scores.

When bone microstructure and μFEA parameters were examined with DXA T-scores, DXA T-scores were significantly correlated with trabecular bone parameters (Tb.N, Tb.Sp, and Tb.BMD) and Ct.Th at the spine, proximal femur, and radius (Table 3). In addition, T-score at the total and ultradistal radius had a significant correlation with Tb.Th and Ct.BMD at the UDR, and with Ct.BMD and Po.Dm at the UDT. In contrast, there was no significant relationship between DXA T-score and Ct.Po at either anatomic site. In μFEA parameters, DXA T-score of all sites had significant correlation with stiffness, apparent modulus, and failure load, such that those with higher T-scores had greater estimated bone strength.

3.2. Comparison of men with normal, low, and osteoporosis-range aBMD.

Of the 78 men studied, 40 had normal aBMD on DXA, 32 had low bone mass on DXA, and 6 had osteoporosis-range aBMD (Table 4). There was no significant difference in age or BMI between the three groups.

At the UDR, men with low bone mass and osteoporotic men had significantly lower Tb.N, higher Tb.Sp, and lower stiffness and failure load than normal men. At the UDT, men with low bone mass and osteoporotic men had lower Tb.N and Tb.BMD, higher Tb.Sp, and lower stiffness and failure load. In addition, men with low bone mass had lower modulus. At both UDR and UDT, there was no significant difference in cortical bone microstructure parameters (Ct.Th, Ct.Po, Po.Dm, and Ct.BMD).

4. Discussion

In the present study, we examined not only the relationships between bone microstructure, aBMD by DXA, FRAX scores, and risk factors for male osteoporosis in healthy men over 50 years old, but also microstructural differences between men with normal, low, and osteoporosis-range aBMD.

Aging is recognized as the most important risk factor for male osteoporosis (Bartl and Frisch, 2009). We observed that age had a correlation with microstructure; cortical porosity and cortical bone mineral density were affected by age, especially at the tibia, a weight-bearing site (Table 2). Our findings were similar to those of Nicks et al. (2012),

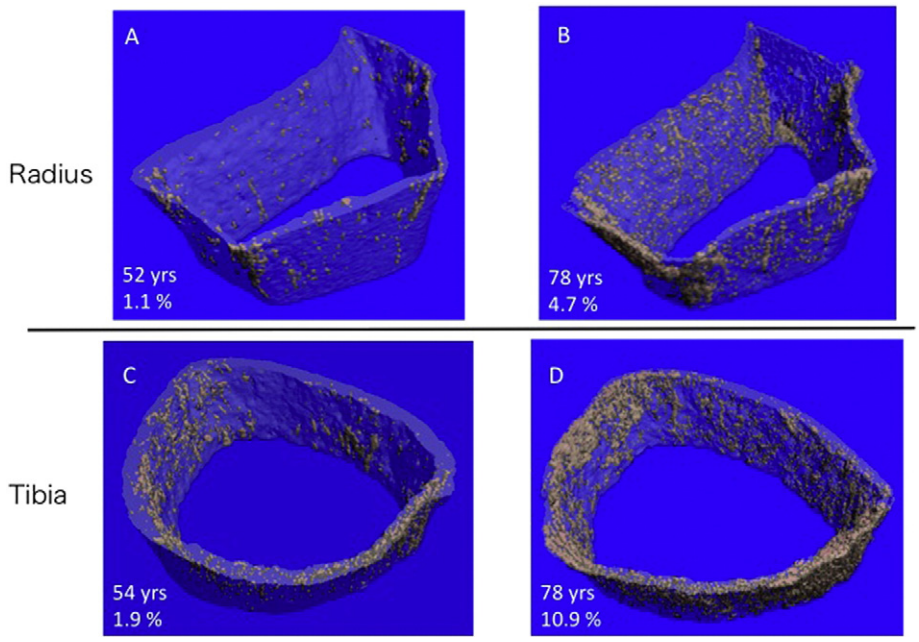

Fig. 1. 3D visualization of cortical bone at the ultra-distal radius (A and B) and tibia (C and D). Intracortical porosity was increase in elderly subjects (B and D).

who compared the bone microstructure of the distal radius and tibia in men under vs. over the age of 50 using HR-pQCT; they reported that cortical porosity was significantly higher in older men, while there was not a significant difference between younger and older men in trabecular bone microstructure. In contrast, when Hansen et al. (2013) reported age-related change of bone microstructure at the radius and tibia in

Table 2
Correlation between DXA T-score and bone microstructure, and age, BMI, serum testosterone, 25(OH)D levels, and FRAX score.

	Age	BMI	Testosterone	25(OH)D	FRAX score	
					Major osteoporotic fracture	Hip fracture
DXA						
L1-L4	0.08	0.13	0.12	0.03	–	–
Total Hip	0.07	0.36 **	0.09	−0.02	–	–
Femoral Neck	−0.03	0.30 **	0.09	−0.07	–	–
Total Radius	−0.09	0.28 *	0.01	−0.12	–	–
1/3 Radius	−0.11	0.25 *	0.03	−0.10	–	–
UDR T-Score	0.00	0.18	0.00	−0.09	–	–
Radius						
Tb.Th	0.04	−0.09	−0.02	0.07	−0.15	−0.16
Tb.N	0.12	0.19	0.11	−0.11	−0.20	−0.27 *
Tb.Sp	−0.17	−0.17	−0.09	0.08	0.20	0.28 *
Tb.BMD	0.11	0.08	0.05	−0.01	−0.22 *	−0.28 *
Ct.Th	−0.02	−0.04	0.15	−0.04	−0.37 **	−0.22
Ct.Po	0.36 **	0.04	−0.09	0.04	0.30 **	0.27 *
Po.Dm	0.26 *	−0.04	0.06	0.18	0.20	0.22
Ct.BMD	−0.18	−0.09	0.16	0.05	−0.27 *	−0.17
Stiffness, *K*	0.04	0.04	0.13	−0.01	−0.50 **	−0.42 **
Modulus, *E*	0.04	−0.03	0.11	0.07	−0.34 **	−0.27 *
Failure load, *F*	0.05	0.06	0.12	−0.03	−0.50 **	−0.44 **
Ct.LF-dis	−0.28 *	0.03	0.10	−0.09	−0.17	−0.06
Ct.LF-prox	−0.25 *	−0.01	0.00	−0.10	0.06	0.20
Tibia						
Tb.Th	0.15	−0.08	−0.04	0.20	−0.04	−0.14
Tb.N	0.24 *	0.33 **	0.00	−0.12	−0.20	−0.18
Tb.Sp	−0.25 *	−0.32 **	−0.01	0.13	0.18	0.19
Tb.BMD	0.30 **	0.22	−0.02	0.06	−0.19	−0.25 *
Ct.Th	−0.11	0.31 **	−0.07	−0.17	−0.46 **	−0.37 **
Ct.Po	0.47 **	0.02	−0.03	0.29 *	0.22	0.20
Po.Dm	0.20	−0.15	0.06	0.29 *	0.18	0.14
Ct.BMD	−0.40 **	0.04	0.07	−0.22 *	−0.34 **	−0.29 **
Stiffness, *K*	0.09	0.22 *	0.02	−0.11	−0.48 **	−0.46 **
Modulus, *E*	0.02	0.15	−0.05	−0.03	−0.35 **	−0.35 **
Failure load, *F*	0.10	0.22 *	0.02	−0.11	−0.47 **	−0.45 **
Ct.LF-dist	−0.48 **	0.19	0.03	−0.30 **	−0.24 *	−0.08
Ct.LF-prox	−0.36 **	0.16	−0.02	−0.22	−0.17	−0.09

Pearson's correlation coefficient $^{*}p < 0.05$, $^{**}p < 0.01$.

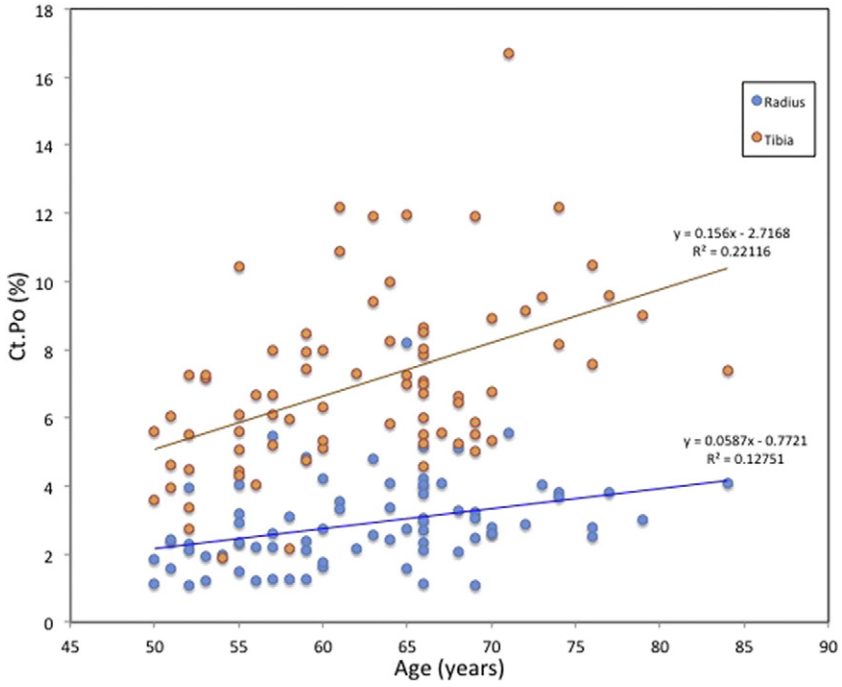

Fig. 2. Correlation between Ct.Po and age. Ct.Po changed significantly with aging, particularly at the tibia.

men aged 20 to 80 years using HR-pQCT, they showed that trabecular bone as well as cortical bone were weakened with aging. In our study, tibial cortical bone microstructure was weakened and load fraction for the cortical compartment was decreasing with aging. Conversely, trabecular bone microstructure became stronger with aging, albeit with a weak correlation. Furthermore, there was no relationship between bone strength and age. Therefore, these findings raise the possibility that while cortical bone is weakened with aging, bone strength is maintained with compensatory strengthening of trabecular bone microstructure. However, our observations were limited to a cohort of men ages 50–84 years.

Aging presumably affects the bones in a number of ways, including telomere shortening (Bekaert et al., 2005), reduced secretion of the sex steroids such as testosterone or estrogen (Khosla et al., 1998), and a decrease in muscle mass (Szulc et al., 2012). We did not observe a significant relationship between serum testosterone levels and bone

Table 3
Correlation between bone microstructure and μFEA parameters, and DXA T-score.

	L-spine	Hip		Radius		
	L1–L4	Total hip	Neck	Total radius	1/3 Radius	UDR
Radius						
Tb.Th	0.12	0.10	0.08	0.44 **	0.21	0.53 **
Tb.N	0.33 **	0.52 **	0.44 **	0.33 **	0.17	0.46 **
Tb.Sp	−0.35 **	−0.54 **	−0.45 **	−0.37 **	−0.19	−0.51 **
Tb.BMD	0.30 **	0.43 **	0.35 **	0.53 **	0.26 *	0.68 **
Ct.Th	0.34 **	0.27 *	0.31 **	0.54 **	0.34 **	0.60 **
Ct.Po	0.01	−0.07	−0.06	−0.11	−0.07	−0.16
Po.Dm	−0.09	−0.05	−0.01	−0.17	−0.08	−0.16
Ct.BMD	0.13	0.12	0.13	0.29 **	0.18	0.38 **
Stiffness, *K*	0.57 **	0.57 **	0.61 **	0.79 **	0.63 **	0.87 **
Modulus, *E*	0.37 **	0.32 **	0.30 **	0.58 **	0.33 **	0.71 **
Failure load, *F*	0.57 **	0.59 **	0.63 **	0.79 **	0.64 **	0.86 **
Ct.LF-dis	0.04	−0.04	0.00	0.04	0.00	0.02
Ct.LF-prox	−0.27 *	−0.33 **	−0.29 *	−0.23 *	−0.22	−0.28 *
Tibia						
Tb.Th	0.12	0.20	0.11	0.16	0.09	0.24 *
Tb.N	0.39 **	0.60 **	0.54 **	0.43 **	0.32 **	0.49 **
Tb.Sp	−0.40 **	−0.60 **	−0.52 **	−0.42 **	−0.31 **	−0.50 **
Tb.BMD	0.43 **	0.64 **	0.53 **	0.48 **	0.33 **	0.59 **
Ct.Th	0.34 **	0.55 **	0.53 **	0.62 **	0.49 **	0.58 **
Ct.Po	−0.04	−0.02	−0.02	−0.16	−0.13	−0.14
Po.Dm	−0.14	−0.15	−0.13	−0.29 **	−0.18	−0.27 *
Ct.BMD	0.18	0.24 *	0.23 *	0.37 **	0.30 **	0.35 **
Stiffness, *K*	0.61 **	0.71 **	0.74 **	0.72 **	0.63 **	0.74 **
Modulus, *E*	0.35 **	0.50 **	0.44 **	0.55 **	0.41 **	0.60 **
Failure load, *F*	0.60 **	0.71 **	0.74 **	0.71 **	0.62 **	0.73 **
Ct.LF-dist	−0.12	−0.06	−0.03	0.05	0.02	−0.02
Ct.LF-prox	−0.19	−0.07	−0.08	0.03	0.02	−0.05

Pearson's correlation coefficient $^{*}p < 0.05$, $^{**}p < 0.01$.

Table 4
Mean values ± SD and differences between normal, osteopenia and, osteoporosis.

Radius	Normal (1) (n = 39)	Osteopenia (2) (n = 32)	Osteoporosis (3) (n = 6)	*p*	
				1 vs 2	1 vs 3
Age (years)	63.1 ± 7.1	62.0 ± 8.3	62.0 ± 9.1	NS	NS
BMI	27.5 ± 3.1	26.9 ± 3.5	25.7 ± 2.3	NS	NS
Tb.Th (μm)	75.0 ± 9.6	74.3 ± 11.9	76.0 ± 15.5	NS	NS
Tb.N (/mm)	2.10 ± 0.22	1.94 ± 0.30	1.77 ± 0.21	*	*
Tb.Sp (μm)	407 ± 54	454 ± 86	498 ± 75	*	*
Tb.BMD (mg/cm^3)	191 ± 31	173 ± 40	158 ± 39	NS	NS
Ct.Th (mm)	1.00 ± 0.16	0.95 ± 0.18	0.88 ± 0.18	NS	NS
Ct.Po (%)	2.9 ± 1.1	2.8 ± 1.4	3.4 ± 1.7	NS	NS
Po.Dm (μm)	172 ± 23	170 ± 17	183 ± 30	NS	NS
Ct.BMD (mg/cm^3)	928 ± 39	923 ± 51	910 ± 53	NS	NS
Stiffness, *K* (kN/mm)	74.4 ± 12.3	64.5 ± 10.6	53.3 ± 11.2	**	**
Modulus, *E* (N/m^2)	1369 ± 248	1226 ± 284	1118 ± 390	NS	NS
Failure load, *F* (N)	4380 ± 679	3829 ± 579	3165 ± 568	**	**
Ct.LF-dis (%)	40.8 ± 7.0	42.1 ± 7.8	38.5 ± 8.3	NS	NS
Ct.LF-prox (%)	77.6 ± 5.1	80.6 ± 6.0	80.8 ± 7.0	NS	NS
Tibia	Normal (1) (n = 40)	Osteopenia (2) (n = 32)	Osteoporosis (3) (n = 6)	*p*	
				1 vs 2	1 vs 3
Age (years)	62.9 ± 7.3	62.0 ± 8.3	62.0 ± 9.1	NS	NS
BMI	27.4 ± 3.1	26.9 ± 3.5	25.7 ± 2.3	NS	NS
Tb.Th (μm)	81.0 ± 10.5	77.8 ± 13.6	77.3 ± 13.3	NS	NS
Tb.N (/mm)	2.07 ± 0.30	1.85 ± 0.26	1.62 ± 0.08	**	**
Tb.Sp (μm)	413 ± 79	476 ± 84	540 ± 38	**	**
Tb.BMD (mg/cm^3)	200 ± 31	171 ± 32	151 ± 29	**	**
Ct.Th (mm)	1.47 ± 0.26	1.34 ± 0.23	1.27 ± 0.37	NS	NS
Ct.Po (%)	6.8 ± 2.5	7.2 ± 2.2	7.6 ± 4.6	NS	NS
Po.Dm (μm)	187 ± 18	193 ± 20	206 ± 52	NS	NS
Ct.BMD (mg/cm^3)	891 ± 53	869 ± 54	867 ± 71	NS	NS
Stiffness, *K* (kN/mm)	188.3 ± 28.1	160.9 ± 21.3	132.9 ± 19.8	**	**
Modulus, *E* (N/m^2)	1709 ± 254	1524 ± 298	1458 ± 469	*	NS
Failure load, *F* (N)	10853 ± 1585	9324 ± 1176	7684 ± 1000	**	**
Ct.LF-dist (%)	43.3 ± 7.1	44.3 ± 7.4	48.1 ± 8.3	NS	NS
Ct.LF-prox (%)	65.4 ± 6.4	67.5 ± 7.1	69.7 ± 9.3	NS	NS

Boneferroni correction, *$p < 0.025$, **$p < 0.005$, NS = not significant.

microstructure, but it has been shown previously that the age-related decline of estrogen has a stronger effect on the bone compared to testosterone (Khosla et al., 2001).

Looker and Mussolino (2008) reported that lower serum vitamin D levels significantly increase the risk of hip fracture in men and women over 65 years old. In that study of people over the age of 65, the prevalence of vitamin D deficiency is high; 26% of them had serum 25(OH)D level under 20 ng/mL (Orwoll et al., 2009). In our study, 30% of all cases had serum vitamin D deficiency (data not shown). We also detected 25(OH)D level had an unexpected modest positive association with cortical porosity, and a negative association with Ct.BMD at the tibia. We suspect that these associations may have been confounded by age, as age was positively associated with both 25(OH)D level ($r = 0.26$, $p = 0.02$, data not shown) and cortical porosity, and negatively associated with Ct.BMD.

Although BMI was weakly correlated with BMD of the hip and radius, it was not correlated with BMD at the lumbar spine (Table 2). Additionally, in microstructure parameters, BMI was weakly correlated with Tb.N, Tb.Sp and Ct.Th in UDT (Table 2). It is reported that BMI is positively associated with BMD of femoral neck in men and women (Lloyd et al., 2014). Furthermore, low BMI is recognized as a risk factor for hip fracture being independent of BMD, while low BMI is not an independent risk factor for the fracture of the other sites (De Laet et al., 2005). In our study, we recognized the relationships between BMI and bone microstructure at the tibia but not at the radius; BMI might have more influence on the bone microstructure at the weight-bearing site than at the non weight-bearing site.

There has been no published report showing the relationship between the FRAX score and bone microstructure. The 10-year probability of a major osteoporotic or hip fracture had significant relationships with cortical parameter, especially at the UDT. Similarly, FRAX score had significant relationships with bone strength. Future research should determine whether cortical bone microstructure and strength may actually improve the predictive ability of the FRAX model or be an alternate tool for fracture risk prediction.

Cortical porosity is attributed to bone resorption on the endocortical surface and on the surface of Haversian and Volkman canals (Keshawarz and Recker, 1984; Zebaze et al., 2010). As the cortical porosity progresses, bone mechanical strength is lowered (Schaffler and Burr, 1988). Nishiyama et al. (2010) compared the microstructure differences between postmenopausal women with normal, low, or osteoporosis-range aBMD; it was shown that women with both low bone mass and osteoporosis had lower Ct.Th and greater Ct.Po. In the present study, we compared men over 50 years old with normal, low, or osteoporosis-range aBMD. Men with osteoporosis and low bone mass had trabecular bone fragility and lower bone strength in both distal radius and tibia; however, there were no significant differences in cortical bone microstructure at the both sites (Table 4). In addition, DXA T-score had no correlation with Ct.Po (Table 3); therefore, DXA is likely not sensitive enough to capture differences in cortical porosity in elderly men. We observed a relatively strong relationship between DXA aBMD and trabecular bone parameters. However, the FRAX score had a stronger relationship with cortical bone parameters compared to trabecular bone parameters, despite the fact that FRAX was calculated from aBMD. A cohort study by Bala et al. (2014) found Ct.Po at the ultra-distal radius was an independent discriminator of forearm fracture in osteopenic, but not osteoporotic women. Therefore, Ct.Po measured by HR-pQCT could provide unique information relevant to fracture discrimination, while trabecular bone microstructure measures may not add significant power beyond aBMD.

This study has several limitations. First, our sample size is small, particularly in the category of men with osteoporosis-range bone mass on

DXA. Second, this was cross-sectional study with men over 50 years of age, which precluded comparisons with a cohort of women, as well as age related changes in bone microstructure. Third, the voxel size of 82 μm is greater than the diameter of some cortical pores and therefore the porosity measures do not reflect small pores; the approach was also limited by the established accuracy and reproducibility of porosity measures using HR-pQCT (Tjong et al., 2012; Burghardt et al., 2010; Nishiyama et al., 2010). However macroscopic porosity is well correlated to integral porosity across all scales (Tjong et al., 2012).

In conclusion, age had a stronger correlation with bone microstructure than other risk factors for male osteoporosis. Cortical bone microstructure was negatively affected by aging, and there was a suggestion that the influence of aging may be particularly important at the weight-bearing sites. Bone strength might be maintained during aging by means of the compensatory strengthening of trabecular bone. When we compared the men with normal, low, and osteoporosis-range aBMD, men with osteoporosis and low bone mass had significantly weak trabecular bone microstructure and bone strength at both the distal radius and tibia, but no significant differences in cortical bone parameters at both sites. Tb.BMD is not really independent of aBMD and therefore will not likely identify those in these groups that are at high risk of fracture. On the other hand, Ct.Po may provide unique discriminatory power in addition to aBMD, based on its poor correlation to aBMD and strong correlation with aging.

Authors' roles

Study design: SM, ALS and AJB. Data collection: NO, AB and KC. Data analysis: NO, AJB and KC. Data interpretation: NO, AJB, KC, ALS and SM. Drafting manuscript: NO. Revising manuscript content: AJB, KC, ALS and SM. Approving final version of manuscript: NO, AJB, KC, ALS and SM. AJB and KC take responsibility for the integrity of the data analysis.

Disclosures

Conflict of interest: The authors declare that they have no conflict of interest.

Acknowledgments

The study was funded by Merck Pharmaceuticals. Additional support was provided by NIH/NIAMS R01 AR060700 to AJB, and the US Department of Veterans Affairs, VHA, CSR&D Service (CDA-2 5 IK2 CX000549), to ALS, SFVAMC.

References

Bala, Y., Zebaze, R., Ghasem-Zadeh, A., et al., 2014. Cortical porosity identifies women with osteopenia at increased risk for forearm fractures. J. Bone Miner. Res. 29:1356–1362. http://dx.doi.org/10.1002/jbmr.2167.

Bartl, R., Frisch, B., 2009. Osteoporosis in Men. Osteoporosis. Springer Berlin Heidelberg, Berlin, Heidelberg, pp. 183–188.

Bekaert, S., Van Pottelbergh, I., De Meyer, T., et al., 2005. Telomere length versus hormonal and bone mineral status in healthy elderly men. Mech. Ageing Dev. 126:1115–1122. http://dx.doi.org/10.1016/j.mad.2005.04.007.

Boyd, S.K., 2007. Accuracy of high-resolution peripheral quantitative computed tomography for measurement of bone quality. Med. Eng. Phys. 29:1096–1105. http://dx.doi.org/10.1016/j.medengphy.2006.11.002.

Boyd, S.K., 2008. Bone strength at the distal radius can be estimated from high-resolution peripheral quantitative computed tomography and the finite element method. Bone 42:1203–1213. http://dx.doi.org/10.1016/j.bone.2008.01.017.

Buie, H.R., Campbell, G.M., Klinck, R.J., Boyd, S.K., 2007. Automatic segmentation of cortical and trabecular compartments based on a dual threshold technique for in vivo micro-CT bone analysis. Bone 41:505–515. http://dx.doi.org/10.1016/j.bone.2007.07.007.

Burghardt, A.J., Kazakia, G.J., Majumdar, S., 2007. A local adaptive threshold strategy for high resolution peripheral quantitative computed tomography of trabecular bone. Ann. Biomed. Eng. 35:1678–1686. http://dx.doi.org/10.1007/s10439-007-9344-4.

Burghardt, A.J., Buie, H.R., Laib, A., et al., 2010. Reproducibility of direct quantitative measures of cortical bone microarchitecture of the distal radius and tibia by HR-pQCT. Bone 47:519–528. http://dx.doi.org/10.1016/j.bone.2010.05.034.

Center, J.R., Nguyen, T.V., Schneider, D., et al., 1999. Mortality after all major types of osteoporotic fracture in men and women: an observational study. Lancet 353: 878–882. http://dx.doi.org/10.1016/S0140-6736(98)09075-8.

De Laet, C., Kanis, J.A., Odén, A., et al., 2005. Body mass index as a predictor of fracture risk: a meta-analysis. Osteoporos. Int. 16:1330–1338. http://dx.doi.org/10.1007/s00198-005-1863-y.

Ebeling, P.R., 2008. Clinical practice. Osteoporosis in men. N. Engl. J. Med. 358:1474–1482. http://dx.doi.org/10.1056/NEJMcp0707217.

Feldkamp, L.A., Davis, L.C., Kress, J.W., 1984. Practical cone-beam algorithm. J. Opt. Soc. Am. A 1, 612–619.

Hansen, S., Shanbhogue, V., Folkestad, L., et al., 2013. Bone microarchitecture and estimated strength in 499 adult Danish women and men: a cross-sectional, population-based high-resolution peripheral quantitative computed tomographic study on peak bone structure. Calcif. Tissue Int. 94:269–281. http://dx.doi.org/10.1007/s00223-013-9808-5.

Hildebrand, T., Laib, A., Müller, R., et al., 1999. Direct three-dimensional morphometric analysis of human cancellous bone: microstructural data from spine, femur, iliac crest, and calcaneus. J. Bone Miner. Res. 14:1167–1174. http://dx.doi.org/10.1359/jbmr.1999.14.7.1167.

Kazakia, G.J., Hyun, B., Burghardt, A.J., et al., 2008. In vivo determination of bone structure in postmenopausal women: a comparison of HR-pQCT and high-field MR imaging. J. Bone Miner. Res. 23:463–474. http://dx.doi.org/10.1359/jbmr.071116.

Keshawarz, N.M., Recker, R.R., 1984. Expansion of the medullary cavity at the expense of cortex in postmenopausal osteoporosis. Metab. Bone Dis. Relat. Res. 5, 223–228.

Khosla, S., Melton, L.J., Atkinson, E.J., et al., 1998. Relationship of serum sex steroid levels and bone turnover markers with bone mineral density in men and women: a key role for bioavailable estrogen. J. Clin. Endocrinol. Metab. 83, 2266–2274.

Khosla, S., Melton, L.J., Atkinson, E.J., O'Fallon, W.M., 2001. Relationship of serum sex steroid levels to longitudinal changes in bone density in young versus elderly men. J. Clin. Endocrinol. Metab. 86:3555–3561. http://dx.doi.org/10.1210/jcem.86.8.7736.

Laib, A., Rüegsegger, P., 1999. Calibration of trabecular bone structure measurements of in vivo three-dimensional peripheral quantitative computed tomography with 28-microm-resolution microcomputed tomography. Bone 24, 35–39.

Laib, A., Hildebrand, T., Häuselmann, H.J., Rüegsegger, P., 1997. Ridge number density: a new parameter for in vivo bone structure analysis. Bone 21, 541–546.

Laib, A., Häuselmann, H.J., Rüegsegger, P., 1998. In vivo high resolution 3D-QCT of the human forearm. Technol. Health Care 6, 329–337.

Lloyd, J.T., Alley, D.E., Hawkes, W.G., et al., 2014. Body mass index is positively associated with bone mineral density in US older adults. Arch. Osteoporos. 9:175. http://dx.doi.org/10.1007/s11657-014-0175-2.

Looker, A.C., Mussolino, M.E., 2008. Serum 25-hydroxyvitamin D and hip fracture risk in older U.S. white adults. J. Bone Miner. Res. 23:143–150. http://dx.doi.org/10.1359/jbmr.071003.

Melton, L.J., Riggs, B.L., van Lenthe, G.H., et al., 2007. Contribution of in vivo structural measurements and load/strength ratios to the determination of forearm fracture risk in postmenopausal women. J. Bone Miner. Res. 22:1442–1448. http://dx.doi.org/10.1359/jbmr.070514.

Morin, S., Lix, L.M., Azimaee, M., et al., 2010. Mortality rates after incident non-traumatic fractures in older men and women. Osteoporos. Int. 22:2439–2448. http://dx.doi.org/10.1007/s00198-010-1480-2.

Mueller, T.L., Christen, D., Sandercott, S., et al., 2011. Computational finite element bone mechanics accurately predicts mechanical competence in the human radius of an elderly population. Bone 48:1232–1238. http://dx.doi.org/10.1016/j.bone.2011.02.022.

Müller, R., Rüegsegger, P., 1995. Three-dimensional finite element modelling of non-invasively assessed trabecular bone structures. Med. Eng. Phys. 17, 126–133.

Müller, R., Hildebrand, T., Häuselmann, H.J., Rüegsegger, P., 1996. In vivo reproducibility of three-dimensional structural properties of noninvasive bone biopsies using 3D-pQCT. J. Bone Miner. Res. 11:1745–1750. http://dx.doi.org/10.1002/jbmr.5650111118.

National Osteoporosis Foundation, 2002. America's bone health: the state of osteoporosis and low bone mass in our nation. Natl. Osteoporos. Found. 1–49.

Nicks, K.M., Amin, S., Atkinson, E.J., et al., 2012. Relationship of age to bone microstructure independent of areal bone mineral density. J. Bone Miner. Res. 27:637–644. http://dx.doi.org/10.1002/jbmr.1468.

Nishiyama, K.K., Macdonald, H.M., Buie, H.R., et al., 2010. Postmenopausal women with osteopenia have higher cortical porosity and thinner cortices at the distal radius and tibia than women with normal aBMD: an in vivo HR-pQCT study. J. Bone Miner. Res. 25:882–890. http://dx.doi.org/10.1359/jbmr.091020.

Orwoll, E., Nielson, C.M., Marshall, L.M., et al., 2009. Vitamin D deficiency in older men. J. Clin. Endocrinol. Metab. 94:1214–1222. http://dx.doi.org/10.1210/jc.2008-1784.

Papaioannou, A., Kennedy, C.C., Cranney, A., et al., 2008. Risk factors for low BMD in healthy men age 50 years or older: a systematic review. Osteoporos. Int. 20: 507–518. http://dx.doi.org/10.1007/s00198-008-0720-1.

Pialat, J.B., Burghardt, A.J., Sode, M., et al., 2012. Visual grading of motion induced image degradation in high resolution peripheral computed tomography: impact of image quality on measures of bone density and micro-architecture. Bone 50:111–118. http://dx.doi.org/10.1016/j.bone.2011.10.003.

Schaffler, M.B., Burr, D.B., 1988. Stiffness of compact bone: effects of porosity and density. J. Biomech. 21, 13–16.

Sornay-Rendu, E., Boutroy, S., Munoz, F., Delmas, P.D., 2007. Alterations of cortical and trabecular architecture are associated with fractures in postmenopausal women, partially independent of decreased BMD measured by DXA: the OFELY study. J. Bone Miner. Res. 22:425–433. http://dx.doi.org/10.1359/jbmr.061206.

Szulc, P., Blaizot, S., Boutroy, S., et al., 2012. Impaired bone microarchitecture at the distal radius in older men with low muscle mass and grip strength. STRAMBO Study 28: 169–178. http://dx.doi.org/10.1002/jbmr.1726.

Tjong, W., Kazakia, G.J., Burghardt, A.J., Majumdar, S., 2012. The effect of voxel size on high-resolution peripheral computed tomography measurements of trabecular and cortical bone microstructure. Med. Phys. 39:1893–1903. http://dx.doi.org/10.1118/1.3689813.

van Rietbergen, B., Odgaard, A., Kabel, J., Huiskes, R., 1996. Direct mechanics assessment of elastic symmetries and properties of trabecular bone architecture. J. Biomech. 29, 1653–1657.

World Health Organization, 1994. Assessment of fracture risk and its application to screening for postmenopausal osteoporosis. Report of a WHO Study Group. World Health Organ. Tech. Rep. Ser. 843, 1–129.

Zebaze, R.M., Ghasem-Zadeh, A., Bohte, A., et al., 2010. Intracortical remodelling and porosity in the distal radius and post-mortem femurs of women: a cross-sectional study. Lancet 375:1729–1736. http://dx.doi.org/10.1016/S0140-6736(10)60320-0.